Published in final edited form as:
Hepatology. 2013 October ; 58(4): 1486–1496. doi:10.1002/hep.26485.

Identification of Intramural Epithelial Networks Linked to Peribiliary Glands that Express Progenitor Cell Markers and Proliferate After Injury

Frank DiPaola[#], **Pranavkumar Shivakumar**[#], **Janet Pfister**, **Stephanie Walters**, **Gregg Sabla**, and **Jorge A. Bezerra**

The Pediatric Liver Care Center and the Division of Pediatric Gastroenterology, Hepatology and Nutrition of Cincinnati Children's Hospital Medical Center, and the Department of Pediatrics of the University of Cincinnati College of Medicine, Cincinnati, OH, USA

[#] These authors contributed equally to this work.

Abstract

Peribiliary glands (PBGs) are clusters of epithelial cells residing in the submucosal compartment of extrahepatic bile ducts (EHBDs). While their function is largely undefined, they may represent a stem cell niche. Here, we hypothesized that PBGs are populated by mature and undifferentiated cells capable of proliferation in pathological states. To address this hypothesis, we developed a novel whole-mount immunostaining assay that preserves the anatomical integrity of EHBDs coupled with confocal microscopy, and found that PBGs populate the entire length of the extrahepatic biliary tract, except the gallbladder. Notably, in addition to the typical position of PBGs adjacent to the duct mucosa, PBGs elongate and form intricate intramural epithelial networks that communicate between different segments of the bile duct mucosa. Network formation begins where the cystic duct combines with hepatic ducts to form the common bile duct, and continues along the common bile duct. The cells of PBGs and the peribiliary network stain positively for α-tubulin, mucins, and chromogranin A, as well as for endoderm transcription factors Sox17 and Pdx1, and proliferate robustly following duct injury induced by virus infection and bile duct ligation.

Conclusion—PBGs form elaborate epithelial networks within the walls of EHBDs, contain cells of mature and immature phenotypes, and proliferate in response to bile duct injury. The anatomical organization of the epithelial network in tubules and the link with PBGs support an expanded cellular reservoir with the potential to restore the integrity and function of the bile duct mucosa in diseased states.

Contact information: Jorge A. Bezerra, Division of Gastroenterology, Hepatology and Nutrition, Cincinnati Children's Hospital Medical Center, 3333 Burnet Avenue, Cincinnati, OH 45229-3030, Phone: 513-636-3008; Fax: 513-636-5581, jorge.bezerra@cchmc.org.
Frank DiPaola – frank.dipaola@cchmc.org
Pranavkumar Shivakumar – pranav.shivakumar@cchmc.org
Janet Pfister – janet.pfister@gmail.com
Gregg Sabla – greggsabla@yahoo.com
Stephanie Walters – stephanie.walters@cchmc.org

Statement Regarding Conflicts of Interest:
The authors have declared no conflicts of interest

Keywords

Bile duct; liver; stem cells; cholestasis; development; regeneration; cholangiocytes

Anatomical and molecular relationships among hepatic and biliary cells are critical to normal development and to the regenerative response following an injury. In the liver, molecular circuits targeting hepatocytes, cholangiocytes, and non-parenchymal cells work coordinately to control embryogenesis and to restore lobular organization and functional integrity after an insult [1, 2]. Although these principles may apply to the development and repair of the intra- and extrahepatic biliary tract, the functional relationships among individual cell types and molecular pathways in bile ducts are less well defined [3]. Recent advances suggest that the embryogenesis of individual segments of the extrahepatic biliary tract (gallbladder, cystic duct, hepatic ducts, and the common bile duct) is regulated at least in part by separate genes, as supported by the isolated defects in mice with mutations in *Inversin, Foxf1*, *Hes1* or *Lgr4* [4-7]. Interestingly, a molecular signature of embryonic endoderm has also been reported in cells of peribiliary glands (PBGs), which appear to have phenotypic plasticity typical of cells with progenitor properties [8].

PBGs are clusters of epithelial cells adjacent to the mucosal lining of intra- and extrahepatic bile ducts, described in several animal species including mice and humans[9-12]. PBG cells express a range of proteins, such as mucins, lysozyme, and pancreatic enzymes, which may be relevant to normal bile duct physiology [13, 14]. In addition, the report that Sox17 and Pdx1 are expressed in PBGs in a fashion that is distinct from the adjacent epithelial lining of fetal bile ducts implies a potential role for PBGs as a niche of multipotent stem cells within the extrahepatic bile duct (EHBD) [8].

Here, we sought further insight into the cellular composition of PBGs and its molecular relationships with the epithelium proper of the duct mucosa. Our working hypothesis was that PBGs are populated by mature and undifferentiated cells capable of proliferation in pathological states. To test this hypothesis, we developed a novel whole-mount in situ immunostaining technique that preserves the anatomical integrity of gallbladder and EHBDs in suckling and adult mice. Applying confocal microscopy and 3-dimensional (3D) reconstruction, we identified PBGs within the submucosal compartment along the entire length of the ductular system, except the gallbladder. Most notably, we discovered that PBGs elongate to form complex epithelial networks that course and branch within the walls, expressing cytokeratin 19, Sox17 and Pdx1 and demonstrating cellular proliferation after viral infection and bile duct ligation.

MATERIALS AND METHODS

Whole-mount staining of EHBDs

The gallbladder, cystic duct and extrahepatic bile ducts of Balb/c mice (Charles River; Wilmington, MA) were microdissected en bloc from mice at 3 and 7 days, and 2 months of age (N=7 in each group); this anatomic unit will be referred to as EHBD, unless otherwise specified. EHBDs were fixed in ice-cold 3.7% formalin for 20 minutes, washed in 1× PBS

for 10 minutes at room temperature (RT), permeabilized in Dent's fixative (80% methanol/20% dimethyl sulfoxide) for 15 minutes, rehydrated through a series of methanol dilutions (75%, 50%, then 25% methanol in distilled H_2O) for 7 minutes per dilution, washed in 1× PBS for 10 minutes and then in diluent solution (1× PBS with 1% bovine serum albumin and 0.1% Triton X-100) for 1.5 hours, followed by blocking in diluent solution containing 10% normal donkey serum for an additional 2 hours and incubation with rabbit-anti cytokeratin (CK) antibody (N1512, undiluted; DAKO North America, Carpinteria, CA) overnight at 4°C. EHBDs were then washed in diluent and incubated in donkey anti-rabbit dylight 488 secondary antibody (711-485-152, diluted 1:333; Jackson Immunoresearch, West Grove, PA) for 5 hours at RT. To complete the assay, EHBDs were washed in diluent and dehydrated in 100% methanol. CK-specific signal using this antibody panel was reproduced using goat anti-mouse CK19 (33111, diluted at 1:100; Santa Cruz Biotechnology, Santa Cruz, CA). The same protocol was applied to the detection of α-tubulin with the addition of antibodies to include mouse anti-α-tubulin (T7451, diluted at 1:333; Sigma Aldrich, St. Louis, MO) and donkey anti-mouse dylight 649 antibody (711-485-152, diluted at 1:333, Jackson Immunoresearch). EHBDs were clarified and imaged in Murray's Clear (2:1 benzyl benzoate:benzyl alcohol) before analysis by confocal microscopy.

Microscopic imaging and 3D renderings

Immunofluorescence and light microscopy imaging was performed using an Olympus BX 51 microscope and attached Olympus DP71 camera. Images were processed with Olympus DP Controller/Manager software. Whole-mount imaging was performed using one of two confocal microscopes as follows: 1) Zeiss LSM 510 on an Axiovert 200M inverted microscope, operating with AIM 4.0 software; or 2) Nikon A1R SI on a Nikon TI-E inverted microscope, operating with NIS Elements 4.0 software. 3D renderings of confocal images were computer-generated using either ZEN 2009 Light Edition or Imaris Version 7.5 software on an HP Z400 Workstation.

Standard immunofluorescence, periodic acid of Schiff's (PAS) and alcian blue staining

EHBDs were snap frozen in OCT medium, sectioned using a cryostat, fixed in ice-cold 3.7% formalin for 20 minutes, and blocked in 10% normal donkey serum. For cytokeratin staining, sections were incubated with undiluted rabbit anti-cytokeratin primary antibody or goat anti-mouse CK19 and a second primary antibody based on the protein of interest, as follows: goat anti-Pdx1 (ab47383, diluted at 1:50000; Abcam, Cambridge, MA), goat anti-Sox17 (AF1924, diluted at 1:2000; R&D Systems, Minneapolis, MN), and rabbit anti-mouse chromogranin A (ID#20085, diluted at 1:5000; Immunostar, Hudson, WI). Cytokeratin antibody incubations were performed for 1 hour at RT, while all other primary antibody incubations were performed overnight at 4°C. To detect specific signals, sections were then counterstained with species-specific antibodies for 1 hour at RT. PAS or alcian blue stainings were performed in paraffin-embedded sections using established protocols [15, 16].

Animals and models of bile duct injury

We injected 1.5×10^6 fluorescence-forming units (ffu) of RRV or 0.9% NaCl (saline) solution intraperitoneally into Balb/c mice within 24 hours of birth, as described

previously [17]. Newborn mice were housed with their mother in a specific pathogen-free vivarium in a room with a 12-hour dark-light cycle. Groups of mice were sacrificed at 3-7 days, and EBHDs were microdissected and snap frozen in liquid nitrogen. All mice received appropriate care that is consistent with criteria outlined in the "Guide for the Care and Use of Laboratory Animals" prepared by the National Academy of Sciences and published by the National Institutes of Health. The Institutional Animal Care and Use Committee of the Cincinnati Children's Research Foundation approved all animal protocols.

Surgical bile duct ligation (BDL) was performed in Balb/c mice at 3 months of age. For the procedure, mice underwent general anesthesia and after a small right subcostal incision the common bile duct was identified, separated from the surrounding tissue, and ligated by deployment of a small titanium ligation clip (LigaClip-LT100; Ethicon Endo-surgery, Cincinnati, OH) in the lower third of the common bile duct. The abdominal cavity was closed by continuous suture of the peritoneal and muscular layers and discontinuous suture of the skin using 5-0 non-absorbable material. The same surgical approach was applied to the sham-operated group, including exposure of the EHBD, except that the bile duct was not ligated. Mice were allowed to wake up and had free access to food and water. At 6, 12, or 24 hours after surgery, 3-4 mice from each group (BDL and sham) were euthanized and the gallbladder, cystic duct and extrahepatic bile ducts were microdissected en bloc as described above.

Staining for cell proliferation by BrdU or EdU incorporation

For measurement of BrdU or EdU uptake, mice were injected intraperitoneally with BrdU (#550891, BD Pharmingen, San Jose, CA) two hours prior to sacrifice, at a dose of 0.1 mg for newborn and 1 mg for adult mice; for EdU incorporation, a dose of 0.3 mg for newborn or 2 mg for adult mice was administered and the detection performed according to the manufacturer's instructions (#C10337, Invitrogen Molecular Probes, Eugene, OR). EHBDs were microdissected from newborn mice at 3 and 4 days of age (N=3-4 for each age for both saline- and RRV-injected groups) and from adult mice at 6, 12, or 24 hours following operation (N=3 for each time point for both sham-operated and BDL mice). All bile ducts were snap frozen in OCT medium, sectioned, fixed in ice-cold 3.7% formalin for 20 minutes. For BrdU detection, bile ducts were subjected to antigen retrieval by incubating in retrieval solution (#550524, BD Retrievagen A; BD Pharmingen), incubated in biotinylated anti-BrdU antibody (#550803, BD Pharmingen) at 1:10 in DAKO antibody diluent overnight at 4°C, and then in dylight 594-conjugated streptavidin (#016-510-084, Jackson Immunoresearch) at 1:1500 in 1×PBS for 1 hour at RT. Slides containing serial sections of EHBDs were coverslipped and examined by fluorescence microscopy. A minimum of 1000 $CK19^+$ main epithelial cells and 200 $CK19^+$ PBG cells were examined per bile duct in each treatment group and, of these, the percentages of $BrdU^+$ or EdU^+ cells in the main epithelium and PBGs were determined by direct observation. A similar protocol was applied to anti-Sox17 and anti-Pdx1 antibodies to identify the dual expression of each protein with CK19+ cells.

Statistical analyses

$BrdU^+$ or EdU^+ cells were expressed as means ± SD and compared between groups using a Welch corrected t test. Statistical significance was set at $P < 0.05$.

RESULTS

PBGs populate the cystic, hepatic and common bile ducts and form intramural epithelial networks

To obtain insight into the cellular composition of PBGs and the potential for shared phenotype(s) with the epithelial lining of the mucosa of bile ducts, we first performed immunofluorescence to detect $CK19^+$ cells in intact EHBDs. In order to define the relationship of PBGs with the epithelium without disrupting the anatomical organization of the intact tissue, we captured serial images from confocal microscopy of whole-mount immunostained EHBDs from 7-day old mice. Analyzing individual photographic frames beginning in the gallbladder and continuing along the ductal system toward the duodenum, we readily identified $CK19^+$ cells forming an intact layer of duct epithelium (Fig 1A). CK staining was also observed in PBGs, which appeared first in the transition between the gallbladder neck and cystic duct (Fig 1A), and remained present throughout the remainder of the ducts (Fig 1B). PBGs and their lumens varied in size. In cystic ducts, they appeared juxtaposed to the epithelium. In the common bile duct, their anatomy was either close to the epithelium or more distinctly separate while maintaining continuity via tubular stalks of variable length (Fig 1A,B).

Analyses of serial sections also identified two additional patterns of PBG anatomy. First, some PBGs appeared not to establish contact with the mucosa epithelium (Fig 2A). Second, we noted the presence of CK19+ tubular structures contained within the wall and displaying a narrow lumen, often parallel to the duct lumen (Fig 2B). To precisely define the anatomic relationship of these seemingly distinct PBGs, we utilized computer software to combine confocal microscopy serial images into 3D renderings of the duct. The reconstitution of these images into a 3D-based duct structure enabled the visualization of unique patterns of organization for PBGs in each major segment of EHBDs. In the cystic duct, PBGs are abundant and the vast majority are single-lobe units that are directly adjacent to the epithelium or connected to it by a short stalk (Fig 3A). Distally, at the union of the cystic and hepatic ducts to form the common duct, some PBGs remain adjacent and connected with the epithelium while others elongate to form tubular structures, coursing through the submucosal compartment (within the wall-boundaries of the duct) and connecting different segments of the ducts (Fig 3B). These structures are formed by two layers of $CK19^+$ cells, vary in the length and may have a lumen, or branch to establish continuity with the neighboring structures (Fig 3B).

At the level of the common duct, PBGs appear larger and some are lobulated, connecting to the epithelium via stalks of varying length or forming tubular structures that may run in parallel to the duct lumen and connect two portions of the common duct (Fig 3C). To examine whether the anatomical organization of PBGs and the peribiliary network varied at the confluence of the common bile duct and the pancreatic duct, we microdissected the bilio-

pancreatic junction and subjected the tissues en bloc to whole-mount immunostaining. We found that the organization and abundance of PBGs and the peribiliary network of the common bile duct are similar to other regions of the duct and completely distinct from the small peripancreatic glands, which communicate largely with the pancreatic duct (not with the common bile duct; Fig 3D; revolving 3D views of each panel in Fig 3 are available as movies accessible in the online supplementary materials – Supplementary Fig. 1A-D). The unique features of PBGs along the different anatomical segments of EHBDs are also present in younger mice (3 days after birth) and adult mice (2 months of age; data not shown). Collectively, these data identify unique patterns of PBG anatomy along different segments of the extrahepatic biliary system and the rich peribiliary networks of $CK19^+$ cells, contained within the wall of the ducts, and most prominent at anastomotic regions and in the common bile duct. The staining of these cells by CK suggested a similar phenotype as that of the neighboring epithelial cells of the duct mucosa, but the unique anatomical organization raised the possibility that they may display other distinct cellular phenotypes.

PBGs and cells of the peribiliary network display markers of differentiation and primitive endoderm

Based on the $CK19^+$ staining detected in individual PBG cells, we first explored whether they express the primary cilium of mature cholangiocytes. Confocal images showed $CK19^+$ PBG cells also expressing α-tubulin similarly to $CK19^+$ cells in the epithelium (Fig 4A,B). α-tubulin (staining the cholangiocyte cilium) is expressed in most but not all PBG cells, as demonstrated by a detailed survey of several EHBDs by serial confocal sections (data not shown). Based on these findings and on previous work reporting the existence of cells producing mucin or expressing other cell markers in PBGs [9, 12], we stained bile duct sections using PAS and alcian blue. Both stains produced similar signals in some but not all PBG cells, but no signal was noted in the duct epithelium (Fig 4C,D). To examine a different type of secretory function, we performed dual staining with CK19 and chromogranin A, which marks neuroendocrine cells, and found that a small population of PBG cells expresses both markers (Fig 4E). A similar staining pattern for all three assays was present in cells of the peribiliary network (data not shown).

Given that PBGs have been proposed to be a niche for multipotent stem cells within the bile duct and the well-described role of the transcription factors Sox17 and Pdx1 in the differentiation of the extrahepatic biliary tree from the endoderm [8, 18], we determined the expression of both of these transcription factors in PBGs along the entire anatomy of gallbladder and EHBDs. Sox17 was expressed predominantly in the gallbladder (61-82% of the epithelial cells of the gallbladder, depending on the age) and less frequently in the cystic duct (3-15% of epithelial cells; 12-30% of PBG cells) and in the common bile duct (<10% of epithelial and PBG cells) (Fig 5A and Fig 6A-C). In contrast, epithelial cells of the gallbladder rarely expressed Pdx1 (<5%), but Pdx1 was expressed in ~50% of the epithelial cells and ~75% of PBG cells of both the cystic duct and common bile duct (Fig 5A and Fig 6A-C). To identify cells with a bilio-pancreatic progenitor phenotype, we also quantified cells that are double stained for Sox17 and Pdx1 ($Sox17^+/Pdx1^+$) in all three segments of EHBDs. We found that $Sox17^+/Pdx1^+$ cells were rare in the gallbladder and represented <20% of epithelial and PBG cells of the cystic duct and common bile duct (Fig 6A-C and

Supplementary Fig 2). Sox17 and Pdx1 signals were also detected in $CK19^+$ cells of the peribiliary network (data not shown). These data suggest that the pattern of expression of endoderm markers in PBGs and the epithelial network is aligned with the expression of the same markers by neighboring mucosal cells, and that there is spatial restriction of such markers to different anatomic subunits of the extrahepatic ductular system (Fig 5B). These findings support the possibility that PBGs and the epithelial network may serve as a reservoir of epithelial cells either to differentiate into or repopulate the mucosa during the regenerative response of the bile duct unit following an injury.

PBGs proliferate in response to epithelial injury and obstructive cholestasis

To directly examine the proliferative potential of PBGs, we quantified cellular proliferation by BrdU uptake in two models of cholestasis. First, we counted the number of $BrdU^+CK19^+$ cells after intraperitoneal administration of RRV into newborn mice. Infection of RRV soon after birth is a well-established injury model of the biliary epithelium and shares phenotypic features of human biliary atresia, the most common cause of chronic cholestatic liver disease in children [19]. We found an unexpectedly high baseline number of BrdU+ positive cells in age-matched controls (receiving saline rather than RRV), both in $CK19^+$ cells of PBG and the peribiliary epithelium and in CK-negative cells in the submucosal compartment of the duct along the entire length of EHBDs (Fig 7). After RRV, the percentage of $BrdU^+CK19^+$ epithelial cells did not change from controls (12±3% vs. 12±2%, P=0.8), neither did PBG cells (7±3% vs. 10±5%, P=0.25) at day 3, but increased in both the epithelium (18±6% vs. 8±3%, P=0.009) and PBGs (20±8% vs. 7±6%, P=0.01) at day 4. These findings are also reproduced when the results of BrdU+ cells are expressed for all epithelial cells together (mucosa + PBGs; Fig 7). We were unable to quantify $BrdU^+CK19^+$ cells reproducibly beyond day 4 because of the widespread epithelial loss that typically begins on day 5 after RRV (data not shown). To investigate if the high baseline BrdU uptake in control newborn mice was due to a normal growth phase of postnatal development, we compared the BrdU uptake by $CK19^+$ cells in ducts of unchallenged neonatal and adult mice. We found that the baseline BrdU uptake decreased in adult mice in both epithelial cells (10±3% neonate vs. 1±1% adult, P<0.0001) and PBG cells (9±6% neonate vs. 1% ±1% adult, P=0.0004; Supplementary Fig 3).

To assess cellular proliferation in adult mice, we quantified $BrdU^+CK19^+$ cells after surgical ligation of the common bile duct. While the percentage of $BrdU^+CK19^+$ cells remained low at baseline levels at 6 and 12 hours after bile duct ligation, $BrdU^+CK19^+$ cells of PBGs and the epithelium underwent a dramatic surge to 39% in PBGs and 33% in the epithelium at 24 hours (P=0.002 and P<0.001, respectively, when compared to sham-operation), or 39% for ligation and 1% for sham when analyzing all cell types collectively for the entire duct (P<0.001; Fig 8). To obtain insight into the degree to which $Sox17^+Pdx1^+$ cells account for this proliferative response, we quantified cells that stained for Sox17, Pdx1 and EdU simultaneously 24 hours after bile duct ligation. In these experiments, we used EdU to label proliferating cells instead of BrdU so that we could optimize the detection of all specific immunofluorescence signals simultaneously; the data for EdU^+ cells when counted as single stainings were similar to $BrdU^+$ cells. We found that $Sox17^+Pdx1^+$ cells accounted for ~50% of the proliferating cells in the cystic duct, but only <10% of the proliferating cells of

the common bile duct (Supplementary Fig 4A-B). Combined, these data clearly show that mucosal and PBG cells are capable of proliferation in response to injuries of the epithelium proper (after RRV infection) and in response to obstruction to bile flow. Notably, the proliferative response involved cells co-expressing $Sox17^+$ and $Pdx1^+$ in the cystic duct, but proliferation in the common bile duct emerged primarily from $Pdx1^+$ cells.

DISCUSSION

We found that PBGs populate the submucosal compartment of the entire extrahepatic biliary system, with the exclusion of the gallbladder. By analyzing the spatial organization of the glands using confocal microscopy to reconstruct the anatomical integrity of the ductular system, we found PBGs to be abundant, small and closely associated with the epithelium in the cystic duct, while they are typically larger in the common duct, at times lobulated and with long stalks connecting to the mucosa. Notably, PBGs also elongate and form ductular structures that interdigitate and create a rich peribiliary network that is contained within the duct wall, predominantly at the sites where the cystic duct joins the hepatic ducts to form the common bile duct. The majority of cells populating this epithelial network stain positive for CK19 and α-tubulin, with a subset of cells staining for mucin and chromogranin A. Despite staining for these markers of differentiated cells, the peribiliary network also expresses Sox17 and Pdx1. However, this expression appears to be tightly linked to the staining in the adjacent mucosa and is dependent on the anatomical region, with Sox17 in gallbladder and cystic duct and Pdx1 in the cystic duct and the common duct. Collectively, these findings show that in addition to typical PBGs, extrahepatic bile ducts contain a previously unrecognized epithelial network that interconnects different segments of bile ducts, with or without a lumen, and generally maintaining contact with the mucosa.

The proposal that the extrahepatic biliary tree is a niche for multipotent stem cells was highlighted recently by the demonstration that biliary cells isolated from human bile ducts express endoderm transcription factors and surface markers of stem/progenitor cells, and can give rise to hepatocytes, cholangiocytes, and beta-islet cells in culture and in vivo [8]. Our results that cells of the peribiliary network express Sox17 and Pdx1 are in keeping with these findings, and recapitulate the documented expression of several other stem cell markers within PBGs [20]. Intriguingly, PBG cells also express markers of fully differentiated cells as supported by the simultaneous expression of CK19 and α-tubulin (for cholangiocytes) and staining for PAS and alcian blue (for mucus-secreting cells). Therefore, peribiliary cells have biomarkers of differentiated cells while retaining markers of early embryogenesis (endoderm) and pancreas. The region-specific expression of Sox17 and Pdx1 by $CK19^+$ cells in gallbladder, peribiliary cells, and/or duct mucosa suggests that the development and function of different segments of the extrahepatic ductular system may be regulated independently. In support of this concept, previous reports have shown that the inactivation of *Inversin* produces atresia of the extrahepatic bile ducts and have patent gallbladder [4] while the inactivation of *Lgr4* induces gallbladder hypoplasia without abnormality in EHBD [6].

Of interest, the proliferation of duct epithelial cells to virus-induced or cholestatic injury was prominent in the mucosa and PBGs throughout the entire EHBD. This proliferative response

did not appear to change the pattern of expression of Sox17 or Pdx1. While we documented that the proliferation occurred in cells that lacked these transcription factors or that expressed either Sox17 or Pdx1, cells co-stained for both Sox17 and Pdx1 accounted for ~50% of the proliferating cells in the cystic duct. This may be a coincidental finding based on our observation that the cystic duct houses cells that express individual transcription factors. Alternatively, the finding may imply that this anatomical region is populated by multipotent cells, and perhaps represent a key source for new cells aiming at the reconstitution of the epithelial compartment after a tissue injury.

The existence of a peribiliary network within the liver and adjacent to intrahepatic bile ducts has been reported by other investigators [21-25]. In these reports, the careful review of consecutive liver sections stained with hematoxylin/eosin identified small single-lobed and larger multi-lobed PBGs, leading to the proposal that they form an intrahepatic peribiliary network with interconnecting PBGs predominantly in areas of duct bifurcation. Intrahepatic PBGs are also capable of proliferation, and have cells that display a differentiated phenotype as demonstrated by the expression of mucins, lactoferrin, and endocrine markers such as somatostatin [11]. Other recent studies suggest that they are likely to be populated by cells expressing endoderm transcription factors such as Sox9 in conjunction with the main duct epithelium, which appear to have the capacity to reestablish differentiated cell populations, including the hepatic parenchyma following injury [26]. Our studies did not address whether cells of intrahepatic PBGs proliferate in response to bile duct ligation or to hepatic injuries. This type of studies requires the modification of the whole-mount staining protocol to the liver, which is a particular challenge due to the large size of the adult liver as a solid organ that is not conducive to penetration of clearing reagents. This limitation notwithstanding, the shared anatomical features of PBGs and the peribiliary network within the intra- and extrahepatic components of the biliary tract support the possibility that PBGs and the peribiliary network constitute niches of multipotent cells within the biliary system that may be involved in the repair of the biliary epithelium [8, 20]. The potential role of PBGs as a reservoir of epithelial cells in the clinical setting was implied by the marked proliferation of PBG cells and hyperplasia of the duct epithelium in patients with hepatolithiasis, cholangitis, and duct ischemia [27, 28]. Directly examining this possibility in an experimental system, we found an increased BrdU uptake in peribiliary cells and the duct mucosa following bile duct ligation (which induces cholangiocyte proliferation without epithelial injury) and after an insult to cholangiocytes by RRV. The proliferative response occurred in a timely manner in peribiliary cells as well as the epithelium of the neighboring mucosa. In both models, neither the anatomical organization of the peribiliary network nor the expression of Sox17 and Pdx1 changed noticeably with BrdU uptake.

In conclusion, our data demonstrate that PBGs elongate to form an elaborate network within the wall of the EHBD, and co-express markers of mature cell types (CK19 and α-tubulin) and transcription factors typically expressed by cells of the endoderm and pancreas. While the interdigitation of epithelial channels (with or without narrow lumen) is more prominent where different anatomical segments unite, they also form ductular structures parallel to the duct lumen, especially along the common bile duct. This unique anatomical organization combined with their ability to robustly proliferate in neonatal and adult mice in response to an injury demonstrate their potential contribution to a regenerative response within the

EHBD. Our data support the concept that PBGs and the peribiliary network are niches of multipotent cells capable of differentiation into multiple cell types to form the ductular system during development, or sites where fully differentiated cells undergo proliferation in response to an insult in order to reconstitute the integrity of the bile duct mucosa.

Supplementary Material

Refer to Web version on PubMed Central for supplementary material.

Acknowledgments

Financial Support:

This work was supported by the NIH grants DK83781 (to J.A.B.), T32 -DK007727 (to F.D.), DK078392 (Integrative Morphology Core of the Digestive Disease Research Center in Cincinnati, to J.A.B.), and a Postdoctoral Research Fellowship Award from the American Liver Foundation/American Association for Studies of Liver Diseases (to F.D.)

Abbreviations

PBGs	peribiliary glands
EHBD	extrahepatic bile duct
RRV	rhesus rotavirus

REFERENCES

1. Lemaigre FP. Mechanisms of liver development: concepts for understanding liver disorders and design of novel therapies. Gastroenterology. 2009; 137:62–79. [PubMed: 19328801]
2. Jia C. Advances in the regulation of liver regeneration. Expert review of gastroenterology & hepatology. 2011; 5:105–21. [PubMed: 21309676]
3. Zong Y, Stanger BZ. Molecular mechanisms of bile duct development. The international journal of biochemistry & cell biology. 2011; 43:257–64. [PubMed: 20601079]
4. Mazziotti MV, Willis LK, Heuckeroth RO, et al. Anomalous development of the hepatobiliary system in the Inv mouse. Hepatology. 1999; 30:372–8. [PubMed: 10421642]
5. Kalinichenko VV, Zhou Y, Bhattacharyya D, et al. Haploinsufficiency of the mouse Forkhead Box f1 gene causes defects in gall bladder development. The Journal of biological chemistry. 2002; 277:12369–74. [PubMed: 11809759]
6. Yamashita R, Takegawa Y, Sakumoto M, et al. Defective development of the gall bladder and cystic duct in Lgr4-hypomorphic mice. Developmental dynamics: an official publication of the American Association of Anatomists. 2009; 238:993–1000. [PubMed: 19301403]
7. Sumazaki R, Shiojiri N, Isoyama S, et al. Conversion of biliary system to pancreatic tissue in Hes1-deficient mice. Nature genetics. 2004; 36:83–7. [PubMed: 14702043]
8. Cardinale V, Wang Y, Carpino G, et al. Multipotent stem/progenitor cells in human biliary tree give rise to hepatocytes, cholangiocytes, and pancreatic islets. Hepatology. 2011; 54:2159–72. [PubMed: 21809358]
9. Burden VG. Observations on the Histologic and Pathologic Anatomy of the Hepatic, Cystic, and Common Bile Ducts. Annals of surgery. 1925; 82:584–97. [PubMed: 17865347]
10. Spitz L, Petropoulos A. The development of the glands of the common bile duct. The Journal of pathology. 1979; 128:213–20. [PubMed: 521865]

11. Nakanuma Y, Katayanagi K, Terada T, Saito K. Intrahepatic peribiliary glands of humans. I. Anatomy, development and presumed functions. Journal of gastroenterology and hepatology. 1994; 9:75–9. [PubMed: 8155872]
12. McMinn RM, Kugler JH. The glands of the bile and pancreatic ducts: autoradiographic and histochemical studies. Journal of anatomy. 1961; 95:1–11. [PubMed: 13774143]
13. Hopwood D, Wood R, Milne G. The fine structure and histochemistry of human bile duct in obstruction and choledocholithiasis. The Journal of pathology. 1988; 155:49–59. [PubMed: 3379517]
14. Terada T, Kida T, Nakanuma Y. Extrahepatic peribiliary glands express alpha-amylase isozymes, trypsin and pancreatic lipase: an immunohistochemical analysis. Hepatology. 1993; 18:803–8. [PubMed: 8406353]
15. Theory and practice of histological techniques. 4th ed. Churchill Livingstone; London: 1996.
16. Sheehan, DC.; Hrapchak, BB. Theory and practice of histotechnology. 2nd ed. The C.V. Mosby Company; St. Louis, MO: 1980.
17. Shivakumar P, Campbell KM, Sabla GE, et al. Obstruction of extrahepatic bile ducts by lymphocytes is regulated by IFN-gamma in experimental biliary atresia. The Journal of clinical investigation. 2004; 114:322–9. [PubMed: 15286798]
18. Spence JR, Lange AW, Lin SC, et al. Sox17 regulates organ lineage segregation of ventral foregut progenitor cells. Developmental cell. 2009; 17:62–74. [PubMed: 19619492]
19. Riepenhoff-Talty M, Schaekel K, Clark HF, et al. Group A rotaviruses produce extrahepatic biliary obstruction in orally inoculated newborn mice. Pediatric research. 1993; 33:394–9. [PubMed: 8386833]
20. Cardinale V, Wang Y, Carpino G, et al. The biliary tree--a reservoir of multipotent stem cells. Nature reviews Gastroenterology & hepatology. 2012; 9:231–40.
21. Nakanuma Y, Sasaki M, Terada T, Harada K. Intrahepatic peribiliary glands of humans. II. Pathological spectrum. J Gastroenterol Hepatol. 1994; 9:80–6. [PubMed: 8155873]
22. Nakanuma Y, Katayanagi K, Terada T, Saito K. Intrahepatic peribiliary glands of humans. I. Anatomy, development and presumed functions. J Gastroenterol Hepatol. 1994; 9:75–9. [PubMed: 8155872]
23. Terada T, Nakanuma Y. Innervation of intrahepatic bile ducts and peribiliary glands in normal human livers, extrahepatic biliary obstruction and hepatolithiasis. An immunohistochemical study. J Hepatol. 1989; 9:141–8. [PubMed: 2809154]
24. Terada T, Nakanuma Y. Development of human intrahepatic peribiliary glands. Histological, keratin immunohistochemical, and mucus histochemical analyses. Lab Invest. 1993; 68:261–9. [PubMed: 7680729]
25. Nakanuma Y. A novel approach to biliary tract pathology based on similarities to pancreatic counterparts: is the biliary tract an incomplete pancreas? Pathol Int. 2010; 60:419–29. [PubMed: 20518896]
26. Furuyama K, Kawaguchi Y, Akiyama H, et al. Continuous cell supply from a Sox9-expressing progenitor zone in adult liver, exocrine pancreas and intestine. Nature genetics. 2011; 43:34–41. [PubMed: 21113154]
27. Kurumaya H, Ohta G, Nakanuma Y. Endocrine cells in the intrahepatic biliary tree in normal livers and hepatolithiasis. Archives of pathology & laboratory medicine. 1989; 113:143–7. [PubMed: 2464976]
28. Sutton ME, op den Dries S, Koster MH, Lisman T, Gouw AS, Porte RJ. Regeneration of human extrahepatic biliary epithelium: the peribiliary glands as progenitor cell compartment. Liver international: official journal of the International Association for the Study of the Liver. 2012; 32:554–9. [PubMed: 22171992]

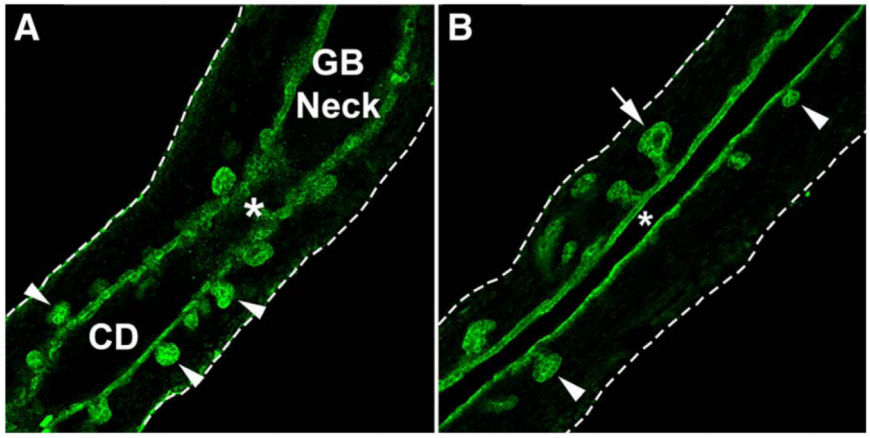

Figure 1. Cytokeratin whole mount immunofluorescence of gallbladder and cystic duct

(A) Two-dimensional (2D) confocal section of the junction between the gallbladder (GB) and cystic duct (CD). PBGs first appear at the transition between the GB and CD, where most PBGs are small and immediately juxtaposed to the mucosa epithelium (arrowheads). (B) 2D confocal section of the common bile duct where PBGs are either immediately juxtaposed to the mucosa epithelium (arrowheads) or connected to the main epithelium via a tubular stalk (arrows). EHBD was obtained from a 7-day old mouse. Green: cytokeratin stain; asterisk: lumen; discontinuous white lines identify the external limits of the GB and ducts.

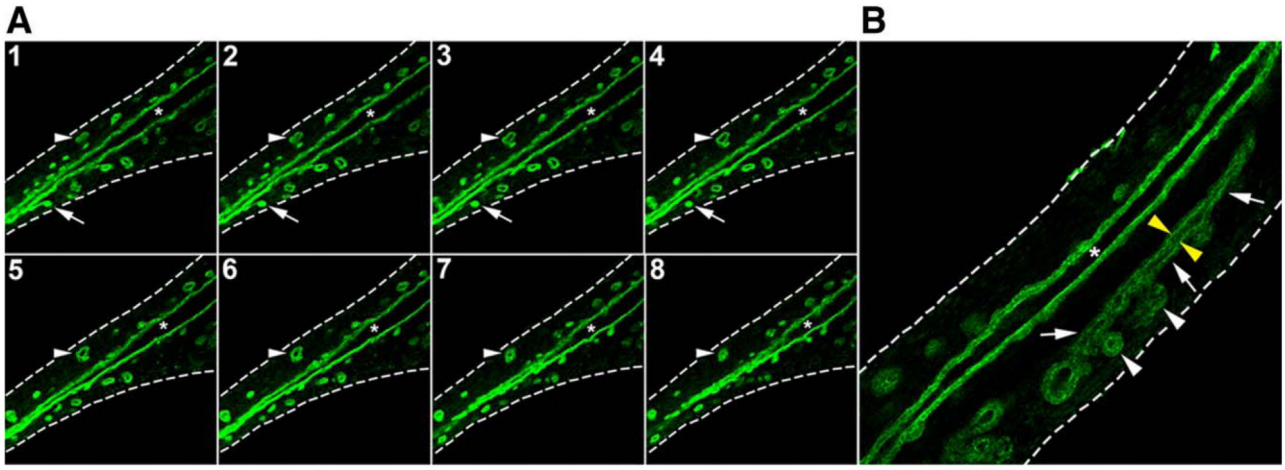

Figure 2. Cytokeratin whole mount immunofluorescence of EHBDs

(A) Serial 2D confocal sections show the common bile duct with multiple PBGs along the mucosa epithelium, some of which appear to connect with the mucosa (white arrows) while others have no obvious link (arrowheads). (B) 2D confocal section showing a tubular structure (white arrows) in the submucosal compartment and contained within the duct wall. The structure courses in parallel to the duct lumen (asterisk), may have adjacent PBGs (white arrowheads), and contains a narrow lumen (yellow arrowheads); discontinuous white lines identify the external limits of the GB and ducts. EHBD was obtained from a 7-day old mouse.

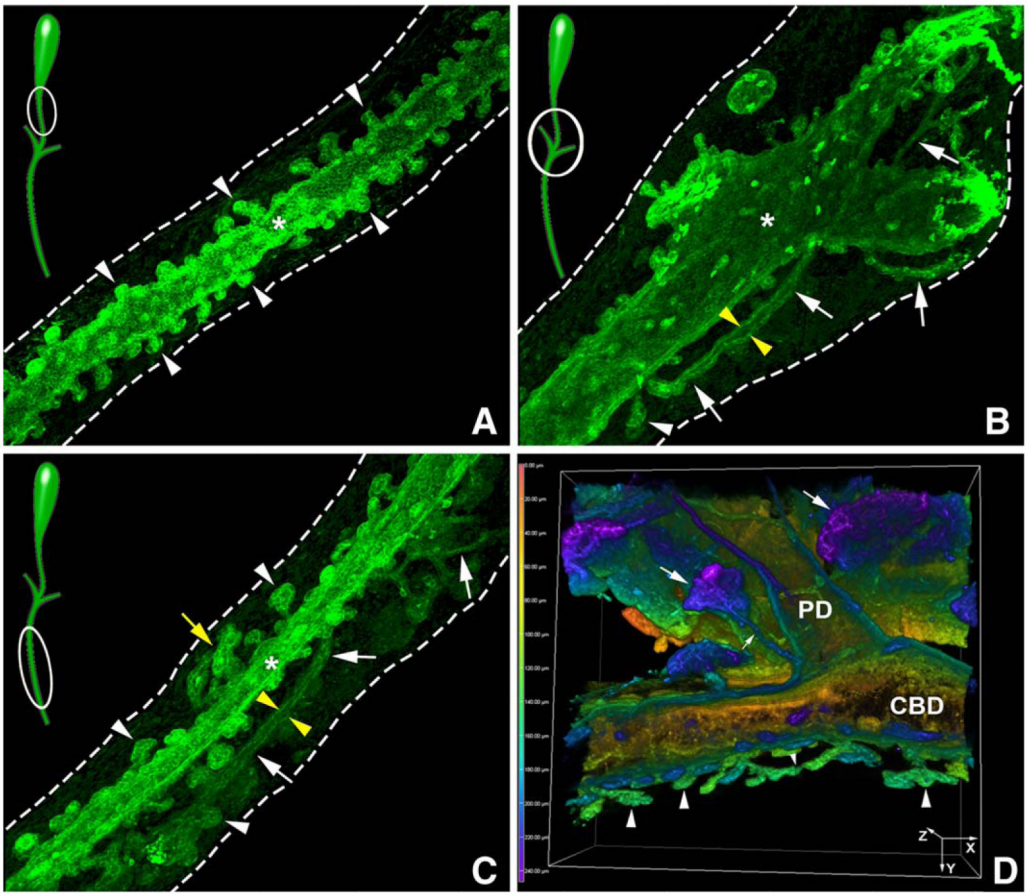

Figure 3. Identification of the peribiliary network

3D rendering of CK19$^+$ EHBDs. In (A), the cystic duct is densely populated by PBGs that are juxtaposed to the mucosa epithelium (white arrowheads). In (B), an intersection of the cystic duct and hepatic ducts to form the common bile duct shows that PBGs either connect with the mucosa or elongate to form a peribiliary network of CK19$^+$ cells (white arrows) within the wall. The network varies in complexity, interconnects different duct segments, and has a narrow lumen (yellow arrowheads) in some areas. In (C), the common bile duct has PBGs that are uni- or multi-lobulated (white arrowhead and yellow arrow, respectively) and connect with the main epithelium, or form the peribiliary network containing tubular structures within the wall (white arrows) and with narrow lumen (yellow arrowheads) connecting different segments of the duct. Discontinuous white lines identify the external limits of the GB and ducts. Asterisk denotes the lumen. In (D), the junction of the common bile duct (CBD) and the pancreatic duct (PD) shows that PBGs and the peribiliary network (in green; arrowheads) are distinct from the pancreatic glands (false-colored in blue based on the depth of field; arrows). EHBD was obtained from a 7-day old mouse.

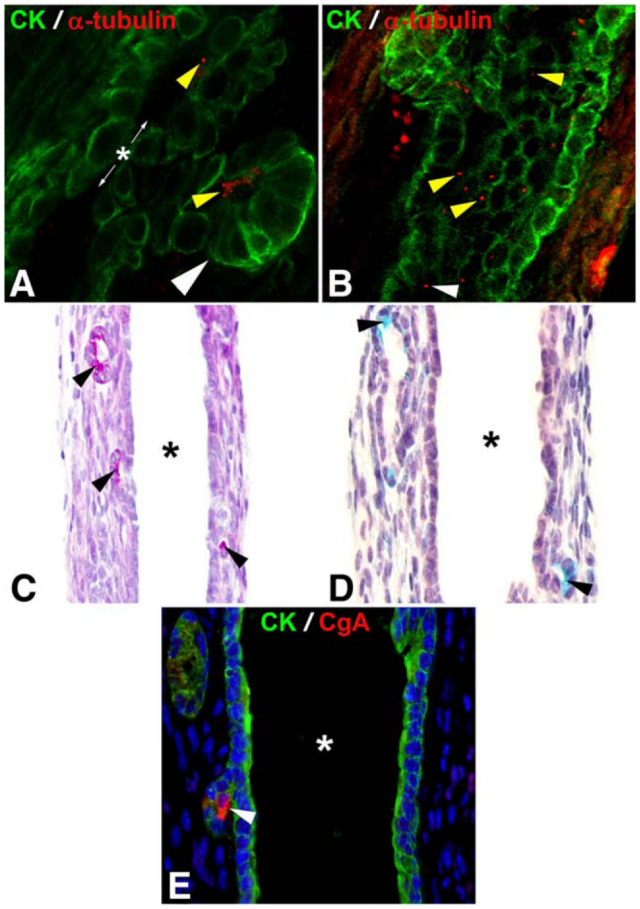

Figure 4. Expression of markers of differentiated cells in PBGs

(A) 2D confocal section showing the duct mucosa and an adjacent PBG (white arrowhead) at high magnification, with α-tubulin signal within the PBG as well as the mucosa epithelium (yellow arrowheads). (B) 2D confocal section showing an additional section of the mucosa epithelium with β-tubulin (yellow arrowheads). (C) PAS and (D) alcian blue stains of paraffin-embedded duct sections label mucins present within the cytoplasm of some PBG cells (arrowheads). (E) Immunofluorescence staining of frozen duct sections using anti-chromogranin A (CgA) antibody reveals cytoplasmic staining within a PBG cell (arrowhead). Asterisk depicts the lumen.

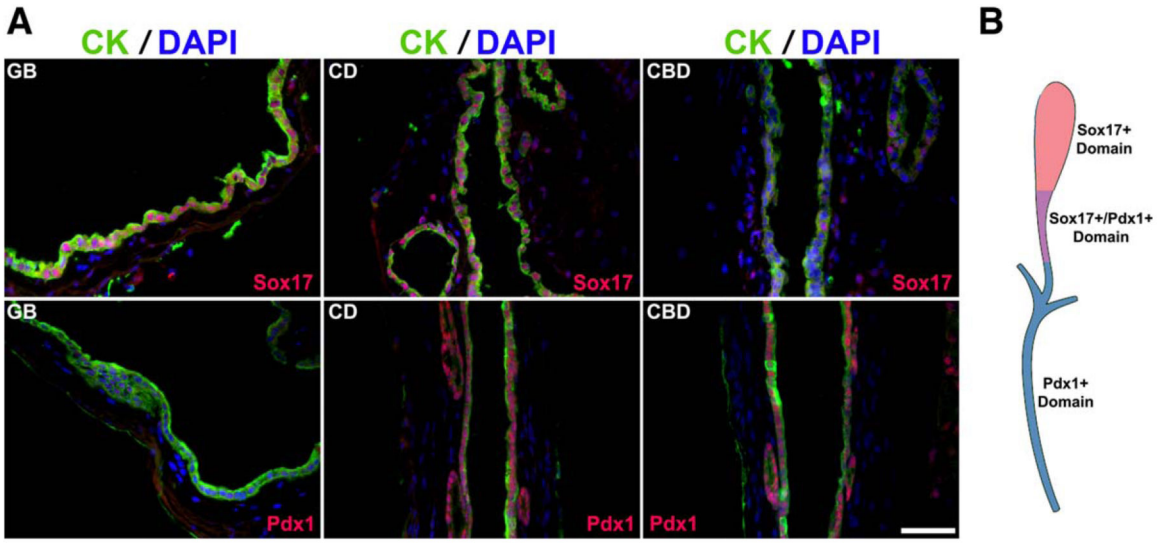

Figure 5. Sox17 and Pdx1 stainings in gallbladders and EHBDs

(A) In the top panel, Sox17 is expressed by the mucosa epithelial cells of the gallbladder (GB) and epithelial cells and PBGs of the cystic duct (CD) but is rarely expressed in the common bile duct (CBD). In the bottom panel, Pdx1 is not expressed in the GB, but is expressed by epithelial cells and PBGs of the CD and CBD. (B) Schematic illustration of the regions of Sox17 and Pdx1 expression in EHBDs. Pink: gallbladder (Sox17 expression). Purple: cystic duct (Sox17 and Pdx1 expression). Blue: intersection and common bile duct (Pdx1 expression).

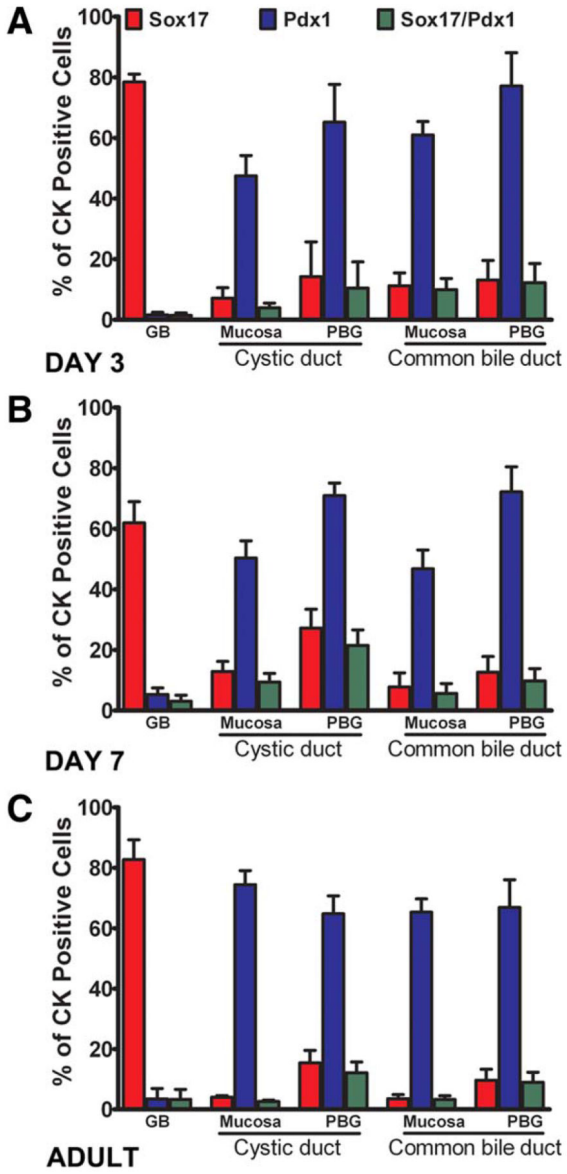

Figure 6. Quantification of Sox17$^+$ and Pdx1$^+$ stained cells

Numbers of cells stained for Sox17, Pdx1 and both Sox17/Pdx1 in different regions of the extrahepatic ductular system at 3 and 7 days and 2 months of age.

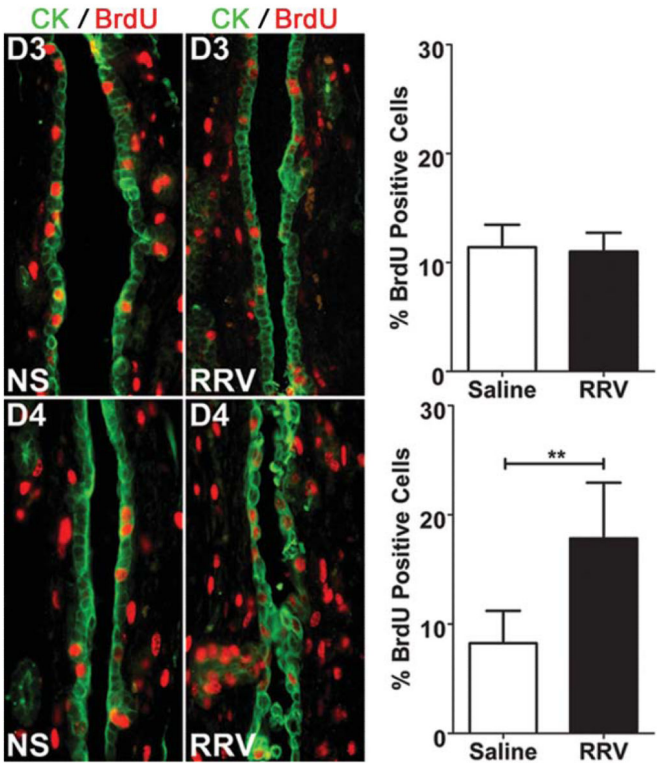

Figure 7. Proliferation of PBGs and mucosa epithelial cells after virus injury

The left panels show $BrdU^+$ cells in extrahepatic bile ducts at days 3 (D3) and 4 (D4) after injection of normal saline (NS) or rotavirus (RRV) into 1 day-old mice. On the right, graphs depict the percent of $BrdU^+CK19^+$ cells (PBGs + mucosa combined), which does not differ between RRV-infected mice and controls at day 3 (D3) after RRV challenge, but increases at day 4 (D4). Results represent the percent of $BrdU^+$ cholangiocytes of PBGs and mucosa combined; NS=normal saline; RRV=rhesus rotavirus; **P<0.01.

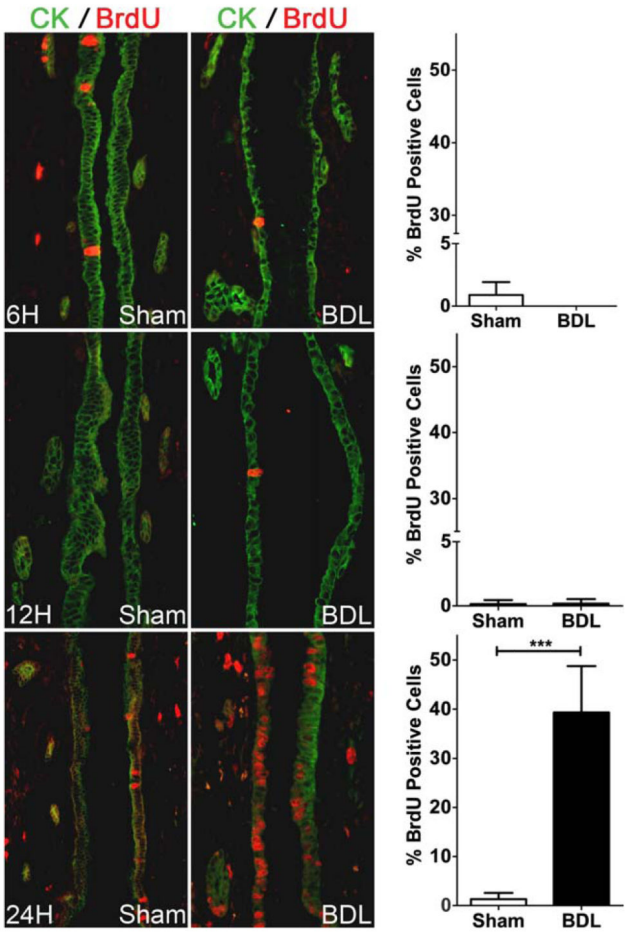

Figure 8. Proliferation of PBGs and mucosa epithelial cells after bile duct ligation

The left panels show BrdU+ cells in extrahepatic bile ducts harvested at 6, 12 and 24 hours after sham operation or bile duct ligation (BDL) of 3 month-old mice. On the right, graphs depict the percent of $BrdU^{+}CK19^{+}$ cells (PBGs + mucosa combined), which does not change at 6 and 12 hours after bile duct ligation (BDL) when compared to sham operation (top and middle graphs), but increases significantly at 24 hours after BDL. Results represent the percent of $BrdU^{+}CK19^{+}$ cells of PBGs and mucosa combined; ***P<0.001.